

# SEGMENTATION OF CORONARY ARTERIAL TREE USING LOCALIZED DEFORMABLE MODEL EMBEDDED WITH AUTOMATED SEEDS

<sup>1</sup>SAMMER ZAI, <sup>2</sup>MUHAMMAD AHSAN, <sup>3\*</sup>YOUNG SHIK MOON

<sup>1,2,3</sup>Hanyang University, Department of Computer Science and Engineering, ERICA Campus, South Korea

\*Corresponding Author

E-mail: <sup>1</sup>sammerzai09@hanyang.ac.kr, <sup>2</sup>ansari05cs04@hanyang.ac.kr, <sup>3\*</sup>ysmoon@hanyang.ac.kr.

## ABSTRACT

This paper presents a fully automatic approach for isolating the left and right coronary arteries from CTA images by embedding our improved fast seed detection method into localized active contour model. Usually active contour based methods require starting point known as seed for their evolution. Accurate provision of this seed point leads to the accurate segmentation. Manual feeding of seed point requires expertise as well as may lead to wrong segmentation. Therefore, in this paper we have combined the quantile and median based thresholded Hessian-based vesselness with that of local geometric features of the vessel to detect the coronary seed points accurately in an automatic fashion. Further, the detected seed points are fed to the active contour model which evolves in a localized way to track the entire coronary arteries to their distal ends. The obtained seed points as well as the obtained segmented left and right coronary arteries are verified by the radiologist at each step. The method is evaluated and validated on nine real clinical CTA datasets and also compared with the previous methods proposed by Lankton et. al and Khedmati et. al. Experimental results reveal that the proposed method outperforms the previous methods qualitatively as well as quantitatively.

**Keywords:** *Computed Tomography Angiography, Coronary arteries, Hessian-based vesselness, Coronary Artery Disease, Deformable Model.*

## 1. INTRODUCTION

Cardiovascular diseases are one of the most important causes of mortality in the industrialized and developing countries [1]. Coronary artery disease (CAD) has become a life threatening disease. The timely diagnosis of such diseases is highly demanded [2]. Hence, an accurate, fast and reliable diagnosis is very important.

For the diagnosis of vascular disorders, segmentation of vasculatures is an indispensable step. Latest imaging modality such as Computed Tomography Angiography (CTA) is one of the most famous imaging tools used for diagnosing the cardiovascular diseases. CTA produces a detailed stack of images whose manual interpretation and analysis by medical experts is quite burdensome and tedious. To lessen the burden of experts, automated or semi-automated segmentation methods are highly required. The segmentation process is one of the pre-processing procedures extensively employed in the imaging field to extract the key features from the given data [3]. Despite

extensive studies, the tracking of coronary arteries still remains a challenging task due to the complex structure of vasculatures and wide inter-patient variability.

Figure 1 describes the anatomical behavior of the heart and the coronary arteries. As shown in Fig. 1(a), the coronary arteries originate from the aorta and are located over the surface of the heart. Coronary arteries are the network of the blood vessels that pump the blood to the myocardium, the heart muscle, to feed it with oxygen nutrients [4]. There are two main coronary arteries: Left Coronary Artery (LCA) and the Right Coronary Artery (RCA). The LCA further splits into Left Circumflex Artery (LCX) and the Left Anterior Descending (LAD). Usually RCA branches into few marginal arteries and Posterior Descending Arteries (PDA).

The anatomical appearance of coronary arteries in CTA data is shown in Fig 1(b), where an axial slice shows the origination of left and right coronary arteries. Figure 1(b) also shows the splitting of left coronary artery into its further branches LAD and LCX.

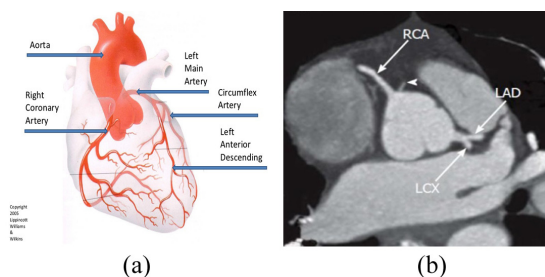


Figure 1: Anatomy of Coronary Arteries

## 2. LITERATURE REVIEW

Despite significant amount of research has already been dedicated towards the segmentation of coronary arteries [5, 6], this area still remains an active research topic. Most of the segmentation methods in the literature are interactive segmentation which requires user involvement and expertise. Segmentation based on the manual interaction from individual users may lead to erroneous segmentation as well as are non-reproducible and they often increase the processing time. To overcome these shortcomings, various techniques have been presented in the literature which addresses the automatic segmentation of coronary arteries.

Shawn Lankton [5] presented an approach for segmenting the coronary arteries using localized energy model. Their method requires an initial seed point manually for each artery separately that is to be used for evolving the contour. The method is simple but may produces leakages during the curve evolution process due to the presence of intensity inhomogeneity in CTA images. Abolfazl Khedmati et al. [7], also proposed a region growing based semi-automatic method for coronary artery segmentation. Their method utilizes the seed re-adjustment criterion for every segment of each coronary artery in order to prevent them to fall into the wrong paths. However, the method requires lots of pre-processing and also finding correct path of artery may fall in a wrong path because of the slight differences in intensities. Another related method has been proposed by Ilkay Oksuz et al. [8] for the isolation of coronary arteries. Their method uses 3D region growing which is followed by pre-processing and vesselness map. To initialize the region growing algorithm, multiple seed points from both right and left coronary arteries are hired. Kitslaar et al. [6] first detected the complete heart section along with aorta followed by region growing method which started in the aorta and halted over the points where candidate components of the coronary tree were found. Bauer et al. [9] presented a generic approach for automatically

detecting tubular objects along with the extraction of their centerlines which were grouped together into tree structures.

By considering the shortcomings of all previously propose methods; there is a need of segmentation method for effectively segmenting the coronary arteries without the need of user involvement. Furthermore, the segmentation method must be able to produce leakage free segmentation.

Therefore, in this paper, we have presented an effective method for segmenting the coronary arterial tree automatically by incorporating our improved seed detection procedure with that of the localized statistical energy model. The seeds are detected on the basis of geometrical feature analysis of the vessel and the vessel probability map. The energy commences its evolvment on the basis of detected seeds for both left and right coronary arteries without involvement of the user.

The paper is organized in four sections. Second 3 discuss the proposed methodology with examples. The experimental results are discussed in Section 4. Lastly, Section 5 concludes the presented work.

## 3. PROPOSED METHOD

The proposed method consists of two steps as shown by the block diagram in Figure 2. The first step comprises of sequence of operations for locating the correct coronary seed points whereas, the second step makes use of the detected coronary seed points and performs the segmentation of both left and right coronary arteries. In this paper, we have extended our work of improved fast seed detection [10] to obtain the final segmentation.

### 3.1 Seed Detection

Active contour model requires initial seed for its further propagation hence providing an initial seed point is a very crucial task for tracking the coronary arteries till their distal ends. Feeding of initial seed points manually may fall into the wrong paths and may also increase the processing time. Therefore, we have adopted our automatic seed detection framework for detecting the initial left and right coronary seeds that will eventually grow in the subsequent step for tracking the coronary arteries to their distal ends.

Firstly, an axial slice consisting of left and right coronary artery components, is selected from a given CTA dataset by using Eq. (1), where  $N$  indicates the total no. of slices present in a CTA volume,  $c_r$  is some constant and  $P$  is the index of the selected axial slice.

$$P = cr * N \quad (1)$$

After selection of an axial slice, the heart region detection technique [11] is applied to detect only the heart region from the chosen slice which is further scrutinized by applying a threshold of -600 HU to keep only the voxels which belong to the heart region and remove the other regions such as lungs.

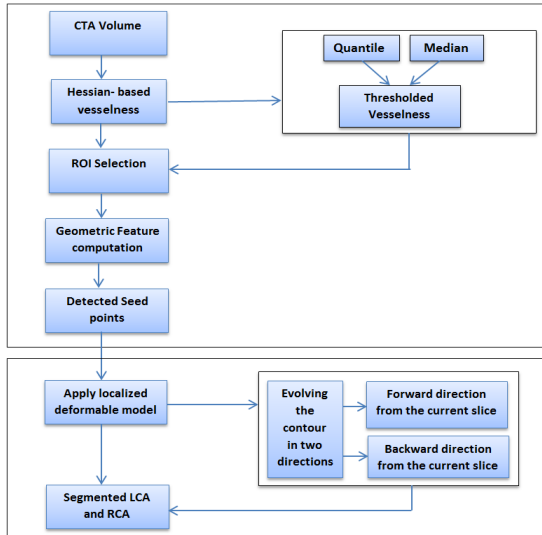


Figure 2: Block Diagram of the Proposed Method

After thresholding, famous Hessian-based vesselness probability map [12] is computed for the obtained restricted domain. However, Hessian-based vesselness measure usually cannot detect vessel features for boundary pixels, because the vessel components at the boundary of the vessel might be a bit narrow than the original ones. Therefore, we have further thresholded the Hessian-based vesselness with respect to quantile and median values. This is done because of the observation that most of the responses in Hessian-based vesselness are zero. Then, sobel edge detector is applied on the resultant data to obtain the edges of the components. Further, contour tracing [13] is performed and the curvature is computed for each of the obtained component by using Eq. (2), where ‘L’ represents the number of pixels belonging to the traced contour, ‘i’ is the index of the current traced pixel and ‘dir’ indicates the direction of the corresponding pixel.

$$K_c = \sum_{i=1}^{L-1} |dir[i+1] - dir[i]| \quad (2)$$

A separate bounding box is created for each of the component and is known as the ROI (Region of Interest) for that vessel candidate. Then for each of the vessel candidate, we compute the local geometric feature by finding out the three parallel vessel cross-sections and generating the UV-planes of indices [-1, 0, 1] which are perpendicular to the direction of the vessel. On each UV-plane, we cast the rays in sixteen uniform directions from their respective center points. Then the border points are computed for each ray by employing the concept of radial gradient and the length of each ray is computed. Further, rays are sorted for each UV-plane with respect to their length and three shortest and three longest rays are removed. For each of the left ray index  $j=[1, \dots, 10]$ , the maximum  $B_{max}[j]$  and minimum  $B_{min}[j]$  values are computed among the three ray lengths. The local geometric feature is computed by using Eq. (3).

$$GF(x) = \prod_{j=1}^{10} \frac{k}{B_{max}[j] - B_{min}[j] + 1} \quad (3)$$

The local geometric feature given in Eq. (3) is incorporated along with the Hessian-based vesselness and the final geometric feature that we have adopted is calculated by using Eq. (4), where  $T_F$  is the threshold used for Hessian-based vesselness and  $T_{GF}$  is the threshold used for the local geometric feature.

$$vesselness(x) = \begin{cases} 1, & \text{if } F(x) \geq T_F \text{ and } GF(x) \geq T_{GF} \\ 0, & \text{otherwise} \end{cases} \quad (4)$$

The vesselness defined by Eq. (4) gives the seeds which are guaranteed to be the coronary components and hence will be used by the subsequent stage of segmentation. Figure 3 shows the selected axial slice and the detected seeds for left and right coronaries.

### 3.2 Segmentation

By using the information of the detected coronary seeds, we start the segmentation of left and right coronary arteries by employing the Chan-Vese deformable model [14] in a localized way. The active contour model makes use of the initial seeds and starts to grow to track the possible coronary arteries.

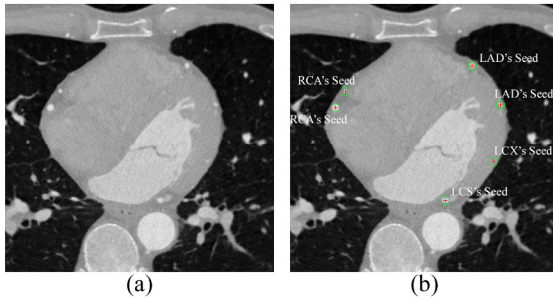


Figure 3: Selection of an Axial Slice and Seed Detection (a) Axial Slice (b) Detection of Initial Coronary Seeds.

The well-known Chan Vese energy formulation as defined in Eq (5) isolates the object from homogenous background on the basis of global mean intensities of inner and outer regions of the contour, respectively. The parameter  $I(x)$  represents the image, whereas,  $c_1$  and  $c_2$  correspond to mean intensities of global interior and global exterior regions, respectively and  $\mu$  length(C) controls the regularity by penalizing the length.

$$F(c_1, c_2, C) = \mu \cdot \text{length}(C) + \int_{\text{inside}(C)} [I(x) - c_1]^2 dx + \int_{\text{outside}(C)} [I(x) - c_2]^2 dx \quad (5)$$

To deal with the intensity variation in CTA images, we use the concept the localization of region based segmentation energies with respect to spatial information. A contour is drawn surrounding the region of interest and then the energy is localized in a way that statistical models of inside and outside regions of the contour become adaptive to the information present in an image. For the localization, a ball function is used to calculate the statistics of the particular region at each point of the curve and is defined by Eq. (6), where 'x' represents the point on the contour and 'y' represents the point present inside the ball having radius 'r' and centered at 'x'.

$$B(x, y) = \begin{cases} 1, & \|x - y\| < r \\ 0, & \text{otherwise} \end{cases} \quad (6)$$

The behavior of the ball drawn at each point of the contour with respect to interior and exterior regions is illustrated by Figure 4.

The curve evolution equation on the basis of localized intensities is defined by Eq. (7), where contour is embedded as a signed distance function

$\phi$ ,  $F$  indicates the image-based force,  $\delta\phi$  denotes the interface at the zero level set and the parameter  $\lambda$  is used for controlling the length of the curve to avoid infinite boundaries.

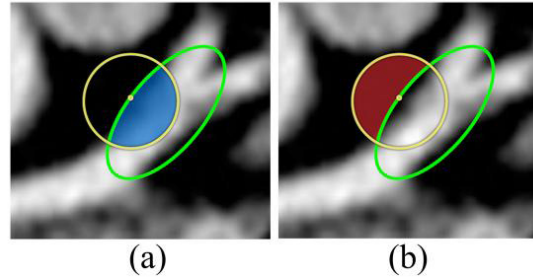


Figure 4: Behavior of Ball Function. (a) Interior Region of the Contour (b) Exterior Region of the Contour.

$$\frac{\partial \phi}{\partial t}(x) = \lambda \delta\phi(x) \int_{\Omega_y} B(x, y) \cdot \nabla_{\phi(y)} F(I(y), \phi(y)) dy + \delta\phi(x) \operatorname{div} \left( \frac{\nabla \phi(x)}{|\nabla \phi(x)|} \right) \quad (7)$$

By incorporating the force in terms of Chan Vese energy in a localized level-set framework, the deformation equation can be expressed as defined by Eq. (8).

$$\frac{\partial \phi}{\partial t}(x) = \delta\phi(x) \int_{\Omega_y} B(x, y) \delta\phi(y) \cdot \left( \frac{(I(y) - c_1)^2}{\int_{\Omega_y} B(x, y) H\phi(y) dy} - \frac{(I(y) - c_2)^2}{\int_{\Omega_y} B(x, y) (1 - H\phi(y)) H\phi(y) dy} \right) + \lambda \cdot \delta\phi(x) \operatorname{div} \left( \frac{\nabla \phi(x)}{|\nabla \phi(x)|} \right) \quad (8)$$

The interior region of the curve is defined by the Heaviside function,  $H\phi$ . It is equal to 1 when  $\phi < 0$ , 0 when  $\phi > 0$ , and has a smooth transition through 0.

#### 4. EXPERIMENTAL RESULTS

This section is dedicated for illustrating the effectiveness of the proposed method. For the accurate isolation of the left and right coronary arteries, the proposed method has been implemented and tested on nine real clinical CTA data sets. The average voxel size of the datasets is  $0.37 \times 0.37 \times 0.36 \text{ mm}^3$ . All images are reconstructed at  $512 \times 512$  size with different number of slices ranging from 250 to 350. For all experiments, we have used 2 to 5 scale range for determining the Hessian-based vesselness measure. The values of thresholds,  $T_F$  and  $T_{GF}$  in Eq. (4), are set to 0.009 and 18, respectively. For computing Eq. (3), the

constant 'k' is set to 2 in our experiments. For the selection of an axial slice, the value of the constant  $c_r$  is used within the range of 0.4 to 0.6. The geometrical feature analysis is carried out on the chosen axial slice followed by median and quantile based thresholding of Hessian-based vesselness. Although, level set approach is popular in representing the contour because of its simple implementation and adaptation towards the topological changes. However, these methods show slow computation. It is therefore, we have adopted sparse field technique developed by Whitaker [15] to implement our proposed algorithm. For a fair comparison with the previously described method [5] we have used the same settings for level set implementation of active contour. The parameter values  $\lambda = 0.1 \max\left(\left|\frac{d\phi}{dt}\right|\right)$  and  $r = 5\text{mm}$  are used

throughout. The choice of  $r$  is reasonable, representing the maximum possible diameter for vessels in the vessel tree [5]. All the experiments were performed using MATLAB on a machine having 2.14 GHz processor with 4 GB RAM.

We show the efficiency of our method with the help of visual results after getting them verified by the radiologist. The average processing time to segment coronary arteries using the proposed method is  $15 \pm 5$  minutes.

Figure 5, shows the detected coronary seeds marked in red color along with the contour evolution process, where the middle row shows the selected axial slice along with the detected seeds. The first row of Fig. 5 consists of three example slices which show the evolution of contours as the slices are navigated in forward direction. Whereas, the last row of Fig. 5 shows the backward progression of contour on three example slices. The utilization of detected seed's information in both directions under the guidance of our thresholded Hessian-based vesselness follows the coronary arteries till their distal ends. There is a possibility that the coronary components are present in the slices exists before and after the selected axial slice used for seed detection. Therefore, we evolve the energy model in two directions in order to grab all the possible coronary components existing in the data. This grabbing of potential coronary components results in the tracking of entire coronary arteries to their distal ends.

The advantage of seed detection procedure is that, unlike Lankton's approach, we do not need to provide seed separately for each artery (LCA and RCA). The detected seeds of the proposed method would be enough to track both arteries completely.

The segmentation results of left and right coronary arteries for three randomly selected CTA volumes are exhibited by Fig. 6, where the performance comparison of the proposed method and the previous methods is shown visually. The first row of Fig. 6 shows the ground truth data obtained by the radiologist, whereas, the segmentation results obtained by Khedmati's and Lankton's approaches are shown by the second and third row, respectively. The superior results of our proposed method are illustrated in the last row of Fig. 6.

By looking at the results of Fig. 6, it can be observed that the proposed method has delineated the coronaries till their potential ends correctly as depicted by the regions enclosed by the green boxes except for a case shown by the blue box, where our method and Lankton's method could not follow the arterial progression till end as compared to Khedmati's result. Although, Khedmati's method works well in such situation due to their seed adjustment procedure during pre-processing stage, but their method is dependent on manual adjustment.

Besides, as illustrated by the third row of Fig. 6, the segmentation of left and right coronaries using Lankton's technique consists of lots of leakages and incomplete structure of arteries due to their intensity based curve evolution procedure. On the contrary, Khedmati's method often suffers from leakages and discontinuities of vessels. Conversely, the vesselness guidance of our method has produced leakage free segmentations along with the possible correct coronary side branches.

For comprehensive evaluation of the proposed, Lankton's, and Khedmati's method, we have computed following parameters, true positive rate (TPR), positive predictive value (PPV) and F-Measure using Eq.(9), (10) and (11). The overall statistical comparison is shown in Table 1. TPR is also known as sensitivity and recall, measures the portion of positive voxels in the ground truth that are also identified as positive by the segmentation being evaluated[16]. PPV is the precision and the parameter F-measure, measures the segmentation accuracy by combining the precision and recall.

$$TPR = \frac{TP}{TP + FN}, \quad (9)$$

$$PPV = \frac{TP}{TP + FP}, \quad (10)$$

$$F - measure = \frac{2 * PPV * TPR}{PPV + TPR} \quad (11)$$

Khedmati's method requires multiple seed points as well as manual adjustment during region growing process, whereas, Lankton's method needs to provide initial seed point individually for each artery to continue its contour based evolution which may require user expertise.

Table 1: Comprehensive Evaluation

	TPR	PPV	F-Measure
Lankton	0.52	0.75	0.62
Khedmati	0.41	0.64	0.46
Proposed	0.83	0.82	0.82

Our proposed method automatically detects the coronary seed points based on the geometrical analysis and hence becomes free from seed adjustment as well as from manual feeding of initial coronary seeds. The statistical data given in Table 1 confirms the superior performance of the proposed method as compared to the Lankton's and Khedmati's approach. Although, Lankton's approach has higher TPR and PPV as compared to Khedmati's method but both of them has lower TPR and PPV value when compared with the proposed method. The proposed method overall achieves 20% and 36% improvements as compared to Lankton's and Khedmati's methods, respectively. The better performance of our method can also be observed by looking at the graph shown in Figure 7.

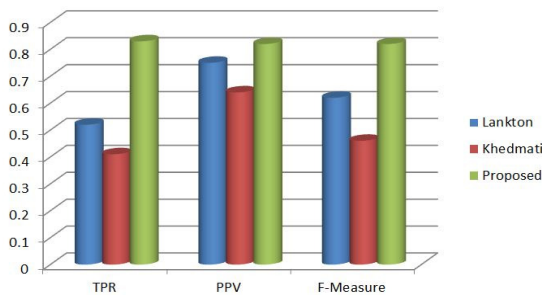


Figure 7: Graph showing TPR, PPV, and F-Measure.

Unlike Khedmati's and Lankton's approach, the proposed method is completely automatic and free from leakages and gaps as shown in Figure 6. The proposed method is highly effective having high TPR, PPV and F-measure as compared to Lankton's and Khedmati's approach, as shown in Table 1 and Figure 7. However, in one instance our method was not able to complete delineate the RCA

up to the distal end as shown by the blue box in Figure 6.

## 5. CONCLUSION

An automatic delineation method has been presented to segment the coronary arteries from CTA data without any user intervention. The method embeds our automatic framework of seed detection within the deformable model. The energy model starts its evolution with automatically detected coronary seeds and deforms locally to track all the possible coronary arteries. The localized energy model is run under the guidance of Hessian-based vesselness in both forward as well as backward direction in order to grab the coronary arteries to their distal ends without any leakage. The proposed method has been tested on nine real clinical CTA volumes and it is found that it effectively produces both of the coronary arteries (LCA and RCA) accurately except for one rare instance where the proposed method was not able to generate RCA up to the distal end. The performance of the proposed method has been shown qualitatively as well as quantitatively. The proposed method is proven to be highly effective in segmenting coronary arteries and does not produce and leakage or gaps. In future, we will test the proposed method on more challenging datasets having severe stenosis and narrowing of vessels. We further plan to employ the proposed method for segmenting coronary arteries for the detection of soft plaque by analyzing the cross-sections of the obtained segmentation at each point of the artery in detail.

## ACKNOWLEDGEMENTS

The authors are highly grateful to Dr. Soon-Yong Song and Dr. Jong-Hyun Lee, department of radiology, Hanyang University Seoul Hospital for provision of the CTA datasets, the ground truth data and their valuable supports throughout the research.

**REFERENCES:**

- [1] Z. Turani, R. A. Zoroofi and S. Shirani, "3D automatic segmentation of coronary artery based on hierarchical region growing algorithm (3D HRG) in CTA data- sets", 2013 20th Iranian Conference on Biomedical Engineering (ICBME), Tehran, 2013, pp. 275-279.
- [2] S. Zai, M.A. Ansari, and Y.S. Moon, "Automatic and effective delineation of coronary arteries from CTA data using two-way active contour model", IEICE Transaction on Information & Systems, Accepted: 2016-12-29.
- [3] M.A. Ansari, S. Zai, and Y.S. Moon, "Performance Comparison of Vesselness Measures for Segmentation of Coronary Arteries in 2D Angiograms", Indian Journal of Science and Technology, Vol. 9, No. 48, 2016.
- [4] J.W. Hole, "Human Anatomy and Physiology", WC Brown, 1990.
- [5] S. Lankton, A. Stillman, P. Raggi, and A. R. Tannenbaum, "Soft plaque detection and automatic vessel segmentation", Proceedings of Medical Image Computing and Computer Assisted Intervention (MICCAI) Workshop: Probabilistic Models for Medical Image Analysis, London, UK, September 2009, pp. 1-9.
- [6] P.H. Kitslaar, M. Frenay, E. Oost, J. Dijkstra, B. Stoel, J.H. Reiber, "Connected component and morphology based extraction of arterial centerlines of the heart (cocomobeach)", In: MICCAI Workshop Grand Challenge Coronary Artery Tracking, The MIDAS Journal, 2008.
- [7] A. Khedmati et al., "Semi-automatic detection of coronary artery stenosis in 3D CTA", IET Image Processing, Vol. 10, No. 10, 2016, pp. 724-732.
- [8] İ. Öksüz et al., "A hybrid method for coronary artery stenoses detection and quantification in CTA images", MICCAI Workshop 3d Cardiovascular Imaging: A MICCAI Segmentation. 2012.
- [9] C. Bauer, H. Bischof, "Edge based tube detection for coronary artery centerline extraction", In: MICCAI Workshop Grand Challenge Coronary Artery Tracking, The MIDAS Journal, 22 Jul 2008.
- [10] S. Zai, M.A. Ansari, S.Y. Song, Y.S. Moon, "Robust Seed Selection for Coronary Arteries Segmentation Using Thresholded Frangi Response", Journal of Electrical Engineering and Computer Science, Accepted: 20.10.2016.
- [11] Y. Wang, "Blood Vessel Segmentation and Shape Analysis for Quantification of Coronary Artery stenosis in CT Angiography", PhD., School of Engineering and Mathematica Sciences, City University, London, 2011.
- [12] A. F. Frangi, W. J. Niessen, K. L. Vincken, and M. A. Viergever, "Multiscale vessel enhancement filtering," PROC. Medical Image Computing and Computer-Assisted Intervention-MICCAI'98, ed: Springer, pp. 130-137, 1998.
- [13] J.R. Parker, "Practical Computer Vision Using C", John Wiley & Sons, New York, USA, 1993.
- [14] T.F. Chan and L.A. Vese, "Active contours without edges", IEEE transactions on Image Processing, Vol. 10, No. 2, January 2001, pp. 266-277.
- [15] R.T. Whitaker, "A level-set approach to 3D reconstruction from range data", International journal of computer vision, Vol. 29, No. 3, September 1998, pp. 203-231.
- [16] M.A. Ansari, S. Zai, and Y.S. Moon, "Automatic Segmentation of Coronary Arteries from Computed Tomography Angiography data cloud using Optimal Thresholding", Optical Engineering, vol.56, no.1, pp.013106-013106, 2017.

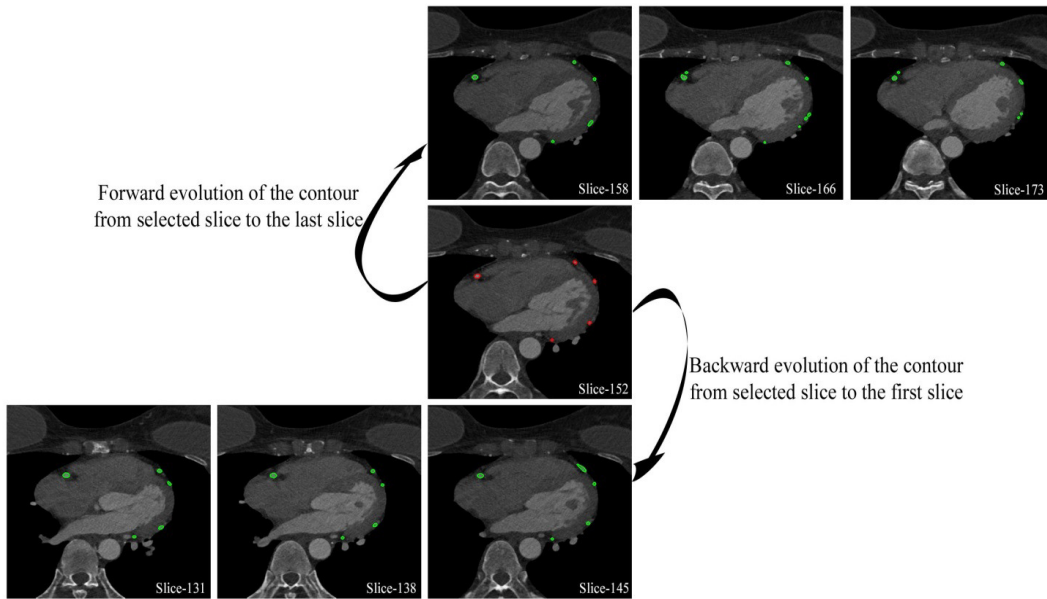


Figure 5: Two-Way Contour Evolution

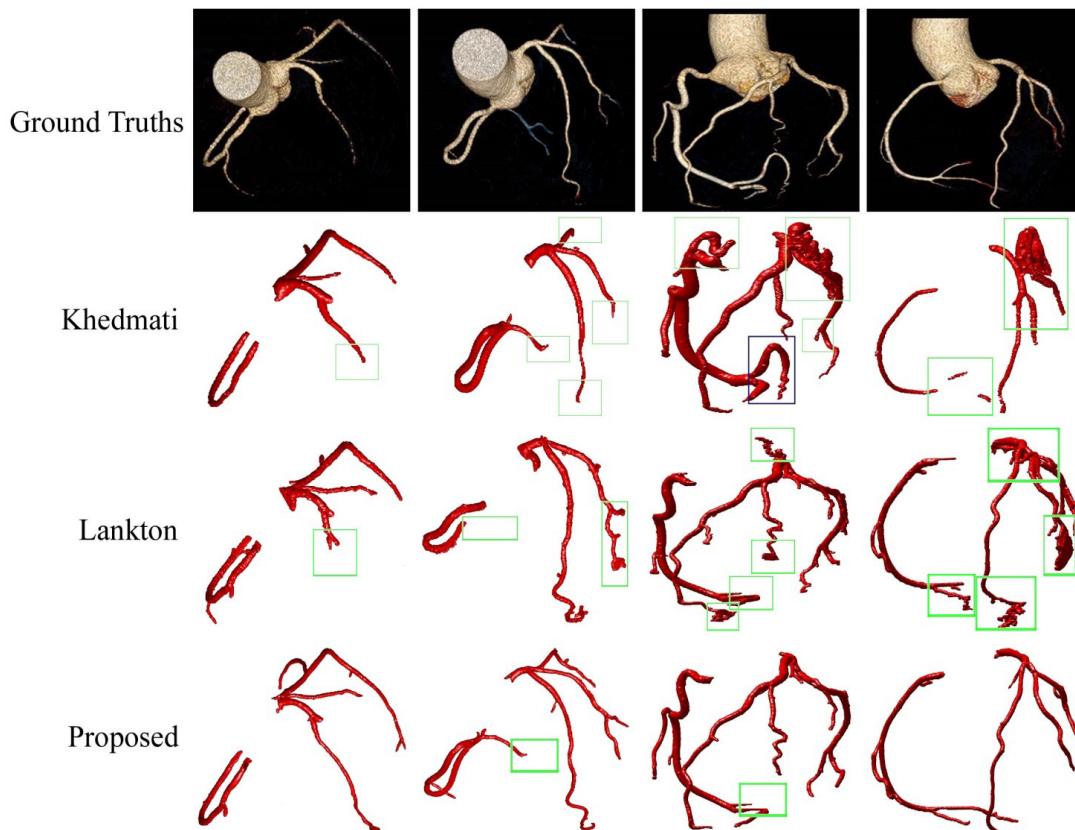


Figure 6: Comparison of Segmentation on Three Randomly Selected Datasets